J Oral Pathol Med (2005) 34: 214–9

www.blackwellmunksgaard.com/jopm

Morphological changes of regional lymph node in squamous cell carcinoma of the oral cavity

Masaya Okura[1], Hajime Kagamiuchi[1], Gyo Tominaga[1], Seiji Iida[1], Yasuo Fukuda[2], Mikihiko Kogo[1]

[1]*The First Department of Oral and Maxillofacial Surgery, Osaka University Graduate School of Dentistry, Osaka;* [2]*Clinical Laboratory, Osaka University Dental Hospital, Osaka, Japan*

BACKGROUND: Regional immune responses with various types of cancer have been studied histopathologically, however, the prognostic value remains conflicting. The aim of this study was to evaluate morphological changes related to lymph node metastasis and the prognostic value for oral cavity squamous cell carcinoma.
METHODS: With histopathologic whole architecture of 430 lymph nodes, gross area, germinal center (GC) area, paracortical area (PA), and tumor area were measured.
RESULTS: Metastatic node had significantly lower distribution ratio of PA to lymphoarea than that of tumor-free node. GC area was not constantly associated with lymph node metastasis. In Cox multivariate analysis, the mean ratio of PA to gross area/lymphoarea was an independent prognostic factor.
CONCLUSIONS: The proportion of PA to gross/lymph area was associated with lymph node metastasis and long-term survival and may be useful in stratification of those patients for a requirement of adjuvant treatments.
J Oral Pathol Med (2005) **34**: 214–9

Keywords: germinal center; head and neck cancer; host immune response; immunosuppression; lymph node metastasis; oral cavity cancer; paracortical hyperplasia; squamous cell carcinoma

Introduction

Cancers of the mouth and pharynx account for 363 000 annual new cases worldwide and almost 200 000 deaths (1). Squamous cell carcinoma (SCC) is the most common neoplasm and comprises approximately 80% of cancers of the oral cavity. Despite optimal treatment, the prognosis of the advanced SCC remains poor. This poor survival is primarily due to a high rate of locoregional failure and secondarily to distant metastases/other malignancy. Incidence of regional lymph node metastases in head and neck cancer is high, and the presence of lymph node metastases is the most important prognostic factor (2, 3). Even when complete surgical resection of primary tumor is possible, a small number of disseminated cells may give rise to local recurrence and metastases. An understanding of the mechanisms, whereby tumor cells are prevented from developing lymph node metastases and tumor cells establish the metastases, is crucial for tumor biology.

Many lymphatic and lymphaticovenous shunts bypass regional lymph nodes and these shunts allow both lymphatic and hematogenous dissemination of malignant cells at an early stage in the vast majority of cancers (4). Chemokine-mediated mechanism seems to be involved with tumor cell invasion into lymph node (5, 6). Regional lymph nodes are considered to have their primary function not merely in anatomic barriers to the systematic dissemination of tumor cells but also in immunologic surveillance (7). A large majority of lymphocytes in lymph nodes are static. When the lymph nodes elicit the immune response, then the nodes enlarge in size (reactive hyperplasia). The immune response can be assessed histologically. The morphological changes indicating a cell-mediated immune response are the development of paracortical hyperplasia and sinus histiocytosis. The morphological change indicating humoral immune response is follicular hyperplasia [germinal center (GC) formation]. The morphological change indicating unstimulated (lymphocyte depletion) is a paucity of lymphocytes in node. Although analysis of histologic lymph node reactivity has been studied on various types of cancer (8–20), the prognostic value of the reactivity is conflicting. The possible reason may be a variety of response patterns in an individual patient as well as in an individual node (21). Some nodes in a patient are static, and others in the same patient frequently have paracortical hyperplasia. The one part of a node is lymphocyte predominant, but the other part of the same node is sometimes lymphocyte depleted. In order to evaluate the immune responses in lymph node, we have developed an image analysis with a digital CCD camera and expressed each immunospecific area numerically.

Correspondence: Masaya Okura, The First Department of OMFS, Osaka University Graduate School of Dentistry, 1–8 Yamadaoka Suita City, Osaka 565-0871, Japan. Tel.: +81-6-6879-2936. Fax: +81-6-6876-5298. E-mail: okura@dent.osaka-u.ac.jp
Accepted for publication October 18, 2004

Table 1 Patient characteristics

Male/female	18/12
Median age (range)	63 (38–82)
Performance status (0–1/2)	25/5
T classification (1/2/3/4)	1/16/11/2
N classification (0/1/2)	8/11/11
Overall stage (II/III/IVA)	5/14/11

Materials and methods

Patient population

Between 1986 and 2000, 312 patients with previously untreated SCC of the oral cavity were treated in our department. Among them, 25 patients received irradiation alone and 89 patients received primary tumor excision alone. About 115 patients, who received preoperative therapies, including induction chemotherapy (22), were also excluded, because these therapies can affect the nodal status. Furthermore, 53 patients with less than five lymph nodes available to evaluate the whole architecture were also excluded, because they received suprahyoidal neck dissection. The remaining 30 patients who received curative surgery with radical, modified, or supraomohyoid neck dissection were enrolled in this study, and a total of 430 lymph nodes were studied. The 30 patients had not any other preoperative therapy. The mean number of nodes evaluated for a patient was 14.3 (range: 5–27). The patient population consisted of 18 (60%) male and 12 (30%) female patients (Table 1). Age ranged from 38 to 82 years, with a median age of 63 years. Tumors were staged using the International Union against Cancer (UICC) classification (23), based on the initial clinical description. Five (16.7%) patients had stage II, 14 (46.7%) patients had stage III, and 11 (36.7%) had stage IVA disease. All patients had biopsy-proven SCC.

Measuring of lymph nodes

All lymph nodes dissected simultaneously for the initial surgery were studied. Histopathologic evaluation of lymph nodes was based on hematoxylin–eosin stained sections prepared by the Pathology Department at the time of the surgery. The whole architecture of each lymph node was evaluated with a microscope (Fluophot plus, Nikon, Tokyo, Japan) and captured with a digital CCD camera (Fuji HC-300, Tokyo, Japan; 1280 × 1000 imaging pixels). The objective (×1; Nikon) was used for capturing whole appearance of the lymph node (Fig. 1). Gross area of node was measured with NIH IMAGE (version 1.62). Area of GCs, more than 250 μm in diameter, was measured, and then deleted (Fig. 1b). The area of GC includes a central paler area and a peripheral annulus of dense small lymphocytes (mantle zone). After additionally removing primary follicles, which ranged 0–0.02 mm^2, paracortical area (PA) was selected with a density slice tool of NIH IMAGE and measured (Fig. 1c). The remaining area contains sinus, medullary cords, and stroma. In case of metastatic lymph node, the area occupied by tumor cells (tumor area) was initially subtracted and measured (Fig. 1d,e). The remaining area, named as lymphoarea (Fig. 1e), was used for measurement of GC area and PA. In an individual node, GC% was calculated with the proportion of GC area to lymphoarea/gross area. PA% was calculated with the proportion of PA to lymphoarea/gross area.

Statistical analysis

The chi-square test (including Yates' correction) or the non-parametric Mann–Whitney *U*-test was used for

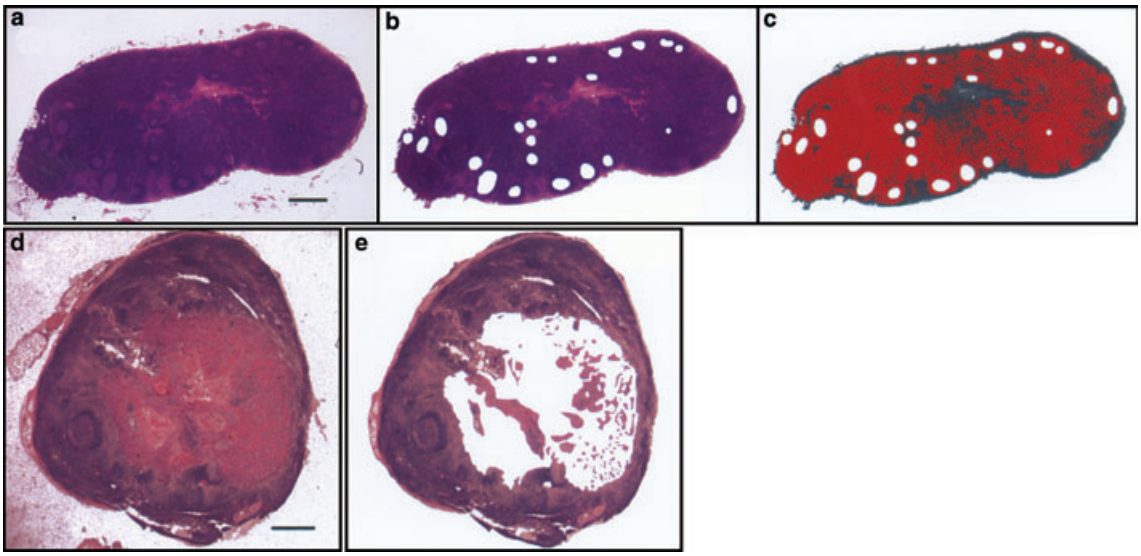

Figure 1 Measuring of lymph node. (a) Whole image of hematoxylin–eosin (H&E) stained tumor-free node with paracortical hyperplasia. Scale bar = 1 mm. (b) After deleting the surrounding tissues of (a), the gross area measured by NIH IMAGE software is 30.7 mm^2. Germinal center (GCs; >250 μm in diameter) have been deleted. The deleted GC area is 1.3 mm^2. (c) Red dots show selected paracortical area (PA) of (a) by a density-slicing tool. The measured PA and PA% is 19.7 mm^2 and 64.2%, respectively. (d) Whole image of metastatic node. The gross area is 33.7 mm^2. Scale bar = 1 mm. (e) Tumor area (9.1 mm^2) of (d) is deleted, and the remaining lymphoarea is 24.6 mm^2. GC area is 0.6 mm^2 and PA is 8.6 mm^2. Calculated GC% and PA% is 2.4% and 35.0%, respectively.

Table 2 Lymph node area (mm^2)

	Gross area	*Lymphoarea*	*Tumor area*
Metastatic nodes ($n = 67$)	81.3 ± 7.6 (8.5–301.7)*	48.0 ± 5.0 (5.3–232.4)*	33.3 ± 4.0 (0.1–138.4)
Tumor-free nodes ($n = 363$)	23.6 ± 1.2 (0.5–139.6)		
No-meta ($n = 119$)	25.4 ± 2.3 (0.5–139.6)**		
Neighbor ($n = 244$)	22.8 ± 1.3 (0.7–137.3)**		

The expressed values are mean ± SE (range).
No-meta, tumor-free nodes in patients with no lymph node metastasis histopathologically; neighbor, tumor-free nodes in patients with lymph node metastasis histopathologically.
*$P < 0.0001$ compared with the gross area of all tumor-free nodes ($n = 363$); **$P = 0.29$ between no-meta nodes and neighbor nodes.

additional analysis for categorical or continuous variables. Cumulative overall survival was calculated by the Kaplan–Meier method and its statistical significance by the log-rank test. Overall survival was measured from the day of initial treatment to death or last known confirmed date alive. Any death (regardless of the cause) was considered as a failure. The univariate and multivariate Cox proportional-hazards models were used to find significant variables for survival. The mean values of GC%, and PA% in each patient were used for the variables. All tests of statistical significance are two-sided.

Results

Lymph node size

Nineteen (63.3%) patients had metastatic lymph nodes, which averaged 3.5 nodes per patient (range: 1–8). A total node number was 430, in which 67 (15.6%) were metastatic nodes with histologic evidence of tumor cells. Metastatic nodes were significantly larger than tumor-free nodes in area (Table 2). A total number of tumor-free lymph node was 363, in which 119 nodes (no-meta nodes) belonged to 11 patients with no lymph node metastasis and 244 tumor-free nodes (neighbor nodes) to 19 patients with lymph node metastasis. The tumor-free nodes were comparable in area between no-meta nodes and neighbor nodes (Table 2). Tumor area occupied by tumor cells in metastatic node averaged 33.3 mm^2 (Table 2). Lymphoarea in metastatic nodes was measured after subtracting the tumor area from the gross area (Fig. 1, see Materials and methods). The lymphoarea in metastatic nodes averaged 48.0 mm^2, more than twofold the gross area of tumor-free nodes (Table 2, $P < 0.0001$), suggesting gross enlargement of metastatic nodes might be attributed to tumor cell invasion as well as some reactive hyperplasia.

Germinal center area

The GC area was comparable between metastatic nodes and tumor-free nodes (Table 3). GC% in metastatic nodes (proportion of GC area to lymphoarea) was marginally ($P = 0.05$) lower than that in tumor-free nodes (proportion of GC area to gross area). The number of nodes without GC was 35 (52.2%) in 67 metastatic nodes, whereas it was 84 (23.1%) in 363 tumor-free nodes (Fig. 2). When those nodes without GC were excluded and the remaining nodes with GC were compared, the GC area of metastatic nodes ($n = 32$) was significantly larger than that of tumor-free nodes ($n = 279$) (Table 3). Hence, half of metastatic nodes represented GC depletion and the remaining half formed GC (follicular hyperplasia).

Paracortical area

The PA% for metastatic nodes was significantly lower than that for tumor-free nodes ($P < 0.001$), although PA was comparable between metastatic and tumor-free nodes (Table 4). The average of PA% was 53.44% for tumor-free nodes, whereas it was 32.3% for metastatic nodes. More than 85% of metastatic nodes had a PA% < 50 (Fig. 3), and those nodes did not represent paracortical hyperplasia. Both PA and PA% were comparable between no-meta and neighbor nodes.

Survival

Median follow-up duration was 59 months, and the 5-year overall survival rate of all 30 patients was 56.9%. Nine died of the disease and three died of other causes with no recurrent disease: suicide, or two other malignancies (esophagus, gall bladder). One patient is currently alive with recurrent disease. By Cox univariate analysis, there was no difference in survival among gender ($P = 0.98$), age ($P = 0.84$), performance status ($P = 0.43$), T classification ($P = 0.79$), or overall stage ($P = 0.17$). In comparison with N0 status, N2 had a marginally poor prognosis ($P = 0.07$). PA% was calculated with the proportion of PA to lymphoarea/gross area in each node, and the mean PA% value of all nodes

Table 3 Germinal center (GC)

	GC area (mm^2)	*GC%*	*GC area of nodes with GC[b] (mm^2)*
Metastatic nodes ($n = 67$)	0.74 ± 0.22 (0–9.79), $P = 0.98$[a]	1.74 ± 0.38 (0–16.91), $P = 0.05$[a]	($n = 32$) 1.54 ± 0.41, $P < 0.05$[a]
Tumor-free nodes ($n = 363$)	0.70 ± 0.06 (0–9.64)	2.66 ± 0.17 (0–18.85)	($n = 279$) 0.92 ± 0.08
No-meta	0.71 ± 0.11 (0–9.64)*	2.96 ± 0.33 (0–17.16)**	0.87 ± 0.13
Neighbor	0.70 ± 0.08 (0–7.12)*	2.51 ± 0.20 (0–18.85)**	0.93 ± 0.10

The expressed values are mean ± SE (range).
*$P = 0.92$ between no-meta nodes and neighbor nodes; **$P = 0.22$ between no-meta nodes and neighbor nodes.
[a]Compared with GC area/GC% of tumor-free nodes (no-meta plus neighbor nodes).
[b]Nodes without GC were excluded, and average values of GC area were calculated in metastatic nodes ($n = 32$) and in tumor-free nodes ($n = 279$).

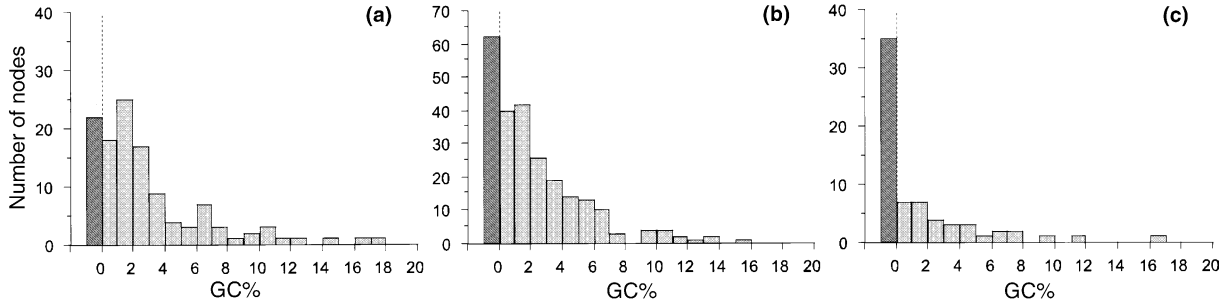

Figure 2 Distribution of germinal center (GC%) in lymph nodes. (a) No-meta nodes ($n = 119$); (b) neighbor nodes ($n = 244$); (c) metastatic nodes ($n = 67$). Dark bars show the number of nodes without GC. Twenty-two (18.5%) no-meta nodes, 62 (25.4%) neighbor nodes, and 35 (52.2%) metastatic nodes had not GC.

Table 4 Paracortical area (PA)

	PA area (mm^2)	*PA%*
Metastatic nodes	13.60 ± 1.43 (0.76–60.05), $P = 0.41$[a]	32.30 ± 2.15 (1.38–79.10), $P < 0.0001$[a]
Tumor-free nodes	12.86 ± 0.72 (0–106.32)	53.44 ± 0.69 (0–96.01)
No-meta	14.14 ± 1.47 (0.24–106.32)*	52.43 ± 1.05 (24.52–76.19)**
Neighbor	12.24 ± 0.79 (0–76.04)*	53.93 ± 0.90 (0–96.01)**

The expressed values are mean ± SE (range).
*$P = 0.21$ between no-meta nodes and neighbor nodes; **$P = 0.31$ between no-meta nodes and neighbor nodes.
[a]Compared with the gross area of all tumor-free nodes ($n = 363$).

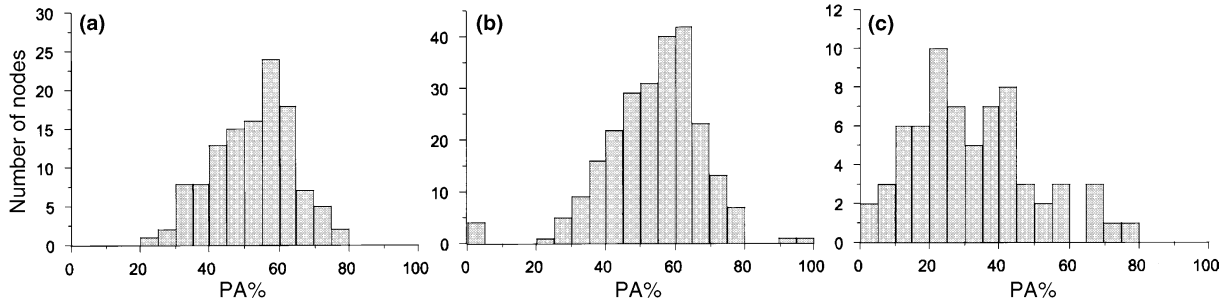

Figure 3 Distribution of paracortical area (PA%) in lymph nodes. (a) No-meta nodes ($n = 119$); (b) neighbor nodes ($n = 244$); (c) metastatic nodes ($n = 67$).

in each patient was calculated for variable of survival. Cox univariate analysis showed that the mean PA% was significantly correlated with overall survival [$P < 0.05$, hazard ratio (HR) = 0.928, 95% CI: 0.871–0.988]. On the contrary, the mean GC% was not significant prognostic factor ($P = 0.74$). After controlling for various confounding factors, the multivariate analysis showed that N classification and mean PA% were an independent prognostic factor (Table 5). The estimated relative rate (e^{β}) is 0.890 for mean PA% (95% CI: 0.811–0.977, $P < 0.05$), indicating that if the mean PA% has a 6% decrease, the risk of death increases two times greater. Mean GC% was insignificant. Fifteen patients (50%, named as high PA group) had more than 50% for the mean PA%, and the remaining 15 patients (low PA group) had < 50%. The adjusted 5-year overall survival for high PA group was 75.2%, significantly superior to that for low PA group (25.2%, Fig. 4a). The estimated relative rate showed that the risk of death for high PA group was 6.7 times lower than that for low PA group ($P < 0.05$). Nine patients in high PA group had metastatic lymph nodes, and 10 patients in low PA group had metastatic nodes. In the subset analysis of those 19 patients with lymph node metastases, the overall survival for high PA group and low PA group was 71.4% and 13.6%, respectively (Fig. 4b).

Table 5 Cox multivariate analysis for relative rates of death by proportional hazards regression

Variables	*Relative rate*	*95% CI*	*P-value*
Mean PA%	0.890	0.811–0.977	0.01
N classification			
N0-referent	1.000		
N1	21.976	0.879–549.280	0.06
N2	31.370	1.605–613.222	0.02

PA, paracortical area; CI, confidence interval.

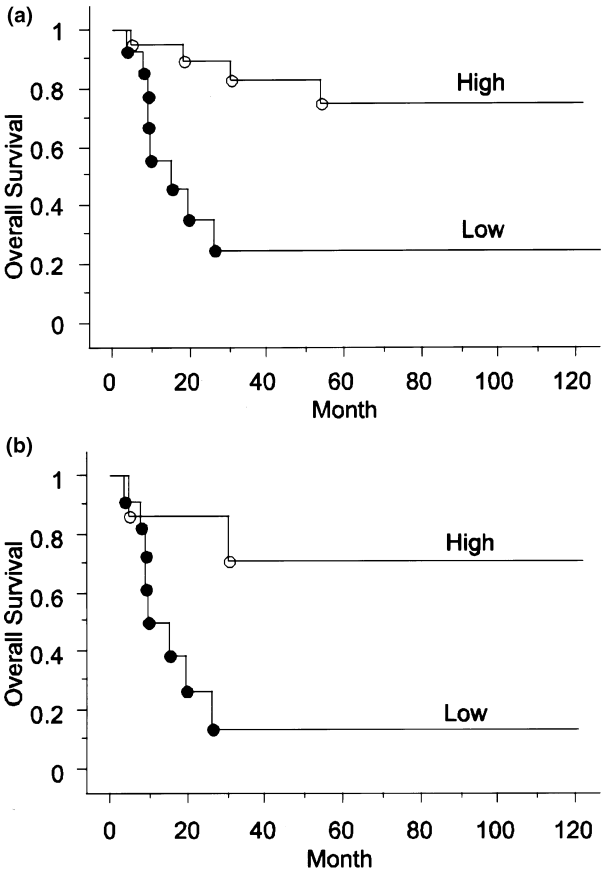

Figure 4 Adjusted overall survival for patients with squamous cell carcinoma (SCC) of the oral cavity. (a) The overall survival curve includes all patients ($n = 30$) both with and without lymph node metastases. The 5-year survival rate for high paracortical area (PA) group ($n = 15$, PA%: $> 50\%$) and low PA group ($n = 15$, PA%: $< 50\%$) was 75.2% and 25.2%, respectively. (b) Overall survival for 19 patients with lymph node metastases. The 5-year survival rate for high PA group ($n = 9$) and low PA group ($n = 10$) was 71.4% and 13.6%, respectively.

Discussion

Several studies have emphasized the important prognostic role of certain immunomorphologic reaction of regional lymph nodes in patients with various types of carcinoma. However, assessing the degree of the immune response has not been objective and has not reached a reproducible result. Some studies (8–12) suggested that paracortical hyperplasia favorably influences survival, some studies (8, 13–16) showed an association between sinus histiocytosis and improved survival, and others (17, 18) said GC predominance was a favorable prognostic factor. Inversely, GC predominance (8, 10, 11, 19), paracortical hyperplasia (20), or sinus histiocytosis (17) was also related with poor survival, similar to lymphocyte depletion. Those conflicting results might be attributed to varying response patterns in an individual patient as well as in an individual node. Indeed, there was node-to-node heterogeneity in the present study. Lymph nodes had a great variety of both cellular and humoral immune responses (Figs 3 and 4). Similarly, the node-to-node heterogeneity of reaction was found with use of [^{3}H]-thymidine uptake from an individual (24). However, there was a disparity between metastatic nodes and tumor-free nodes. It is a well-established fact that metastatic nodes are usually larger than tumor-free nodes in size, while tumor cells have sometimes metastasized in small nodes. The mean gross area of metastatic nodes was 3.5-fold mean gross area of tumor-free nodes and the mean lymphoarea of metastatic nodes was twice of tumor-free nodes. Therefore, the enlargement of metastatic nodes was attributed to tumor cell invasion as well as increase of lymphoarea. In comparison with tumor-free nodes, humoral immune response was suppressed in half of metastatic nodes, and the remaining half metastatic nodes were considered as follicular hyperplasia (Fig. 2, Table 3). Hence, the development of GC is not constantly associated with tumor cell progression in lymph node, and there is not likely regular pattern. On the contrary, suppression of cellular immune response, in particular T cell, correlated to lymph node metastasis. Although lymphoarea in metastatic nodes had enlarged, PA was the similar size to tumor-free nodes. As a result more than 85% of metastatic nodes had low PA%, suggesting the immune activity of T cell is relatively low. Consistent with the finding tumor progressive growth seems to eventually induce the generation of a state of cellular-mediated immunosuppression in the tumor draining lymph nodes (25–27), and the mechanism of tumor-induced immunosuppression has been suggested by the induction of apoptosis of T lymphocytes (28, 29).

Several studies revealed surface marker expression of lymph node mononuclear cells with flow cytometry analysis. Within gated lymphocyte population of regional tumor-free nodes in patients with head and neck cancer, 41–56% was shown to be CD3-positive T cell (27, 30, 31). The T-cell population is similar to our measured PA% (53.4%). In immunohistochemical analysis, Maneses et al. (32) demonstrated that CD3-positive T-cell area was 25–35% of the largest tumor-free lymph node in patients with head and neck SCC. In all those studies one or two lymph nodes were examined for each patient. Such analyses can be definitely accomplished for T cell. However, there is node-to-node heterogeneity and our study aims at evaluating all lymph nodes. We study all lymph nodes with using X1 objective in order to capture those whole architecture. Although the low magnification image does not allow us to distinguish sinus histiocytosis from lymphocyte depletion. Our image analysis is simple and has no need of equipment such as FACScan.

Cox multivariate analysis revealed that the mean PA% was associated with long-term survival, although the number of patients was small. The 5-year corrected survival rate for patients with high mean PA% ($> 50\%$, $n = 15$) was significantly superior to those with low mean PA% ($< 50\%$, $n = 15$). Even when we exclude from our analysis all patients with no metastatic nodes ($n = 11$), the difference of the overall survival rates between high mean PA% group ($n = 9$) and low mean PA% group ($n = 10$) were statistically significant. Our

observations suggest the possibility that cellular immune response, in particular T-cell function, plays a key role in developing lymph node metastasis and the mean PA% is a useful prognostic factor in predicting survival in patients with SCC of the oral cavity.

References

1. Parkin DM, Pisani P, Ferlay J. Global cancer statistics. *CA Cancer J Clin* 1999; **49**: 33–64.
2. Shah JP, Medina JE, Shaha AR, Schantz SP, Marti JR. Cervical lymph node metastasis. *Curr Probl Surg* 1993; **30**: 284–335.
3. Okura M. Lymph node metastasis. In: Pandalai SG, ed. *Recent research developments in cancer*. Vol. 4, Part 1. Trivandrum, India: Transworld Research Network, 2002; 331–7.
4. Cady B. Lymph node metastases. Indicators, but not governors of survival. *Arch Surg* 1984; **119**: 1067–72.
5. Delilbasi CB, Okura M, Iida S, Kogo M. Investigation of CXCR4 in squamous cell carcinoma of the tongue. *Oral Oncol* 2004; **40**: 154–7.
6. Muller A, Homey B, Soto H, et al. Involvement of chemokine receptors in breast cancer metastasis. *Nature* 2001; **410**: 50–6.
7. Santin AD. Lymph node metastases: the importance of the microenvironment. *Cancer* 2000; **88**: 175–9.
8. Di Giorgio A, Mingazzini P, Sammartino P, Canavese A, Arnone P, Scarpini M. Host defense and survival in patients with lung carcinoma. *Cancer* 2000; **89**: 2038–45.
9. Amar A, Rapoport A, Rosas MP. Evaluation of lymph node reactivity in differentiated thyroid carcinoma. *Sao Paulo Med J* 1999; **117**: 125–8.
10. Stankiewicz C. Prognostic significance of lymph node reactivity in patients with laryngeal carcinoma. *Eur Arch Otorhinolaryngol* 1994; **251**: 418–22.
11. Ring AH, Sako K, Rao U, Razack MS, Reese P. Immunologic patterns of regional lymph nodes in squamous cell carcinoma of the floor of the mouth. Prognostic significance. *Am J Surg* 1985; **150**: 461–5.
12. Pihl E, Malahy MA, Khankhanian N, Hersh EM, Mavligit GM. Immunomorphological features of prognostic significance in Dukes' Class B colorectal carcinoma. *Cancer Res* 1977; **37**: 4145–9.
13. Di Giorgio A, Botti C, Mingazzini P, Canavese A, Arnone P. Gastric cancer: prognosis and lymph node reactivity. *Eur J Surg* 1995; **161**: 575–80.
14. Gallo O, Boddi V, Bottai GV, Franchi A, Storchi OF. Prognostic significance of clinically false positive cervical lymph nodes in patients with laryngeal carcinoma. *Cancer* 1995; **75**: 1077–83.
15. Patt BS, Close LG, Vuitch F. Prognostic significance of sinus histiocytosis in metastatic laryngeal cancer. *Laryngoscope* 1993; **103**: 498–502.
16. Hunter RL, Ferguson DJ, Coppleson LW. Survival with mammary cancer related to the interaction of germinal center hyperplasia and sinus histiocytosis in axillary and internal mammary lymph nodes. *Cancer* 1975; **36**: 528–39.
17. Cernea C, Montenegro F, Castro I, et al. Prognostic significance of lymph node reactivity in the control of pathologic negative node squamous cell carcinomas of the oral cavity. *Am J Surg* 1997; **174**: 548–51.
18. Black MM, Freeman C, Mork T, Harvei S, Cutler SJ. Prognostic significance of microscopic structure of gastric carcinomas and their regional lymph nodes. *Cancer* 1971; **27**: 703–11.
19. Check IJ, Cobb M, Hunter RL. The relationship between cytotoxicity and prognostically significant histologic changes in lymph nodes from patients with cancer of the breast. *Am J Pathol* 1980; **98**: 325–38.
20. Syrjanen KJ. Paracortical activity in the lymph nodes draining female breast carcinoma. *Neoplasma* 1979; **26**: 95–102.
21. Cochran AJ, Pihl E, Wen DR, Hoon DS, Kone EL. Zoned immune suppression of lymph nodes draining malignant melanoma: histologic and immunohistologic studies. *J Natl Cancer Inst* 1987; **78**: 399–405.
22. Okura M, Hiranuma T, Adachi T, et al. Induction chemotherapy is associated with an increase in the incidence of locoregional recurrence in patients with carcinoma of the oral cavity: results from a single institution. *Cancer* 1998; **82**: 804–15.
23. Sobin LH, Wittekind C. *UICC International union against cancer 1997. TNM classification of malignant tumours*, 5th edn. Tokyo, Japan: Kanehara & Co., Ltd, 1997.
24. Hoon DS, Korn EL, Cochran AJ. Variations in functional immunocompetence of individual tumor-draining lymph nodes in humans. *Cancer Res* 1987; **47**: 1740–4.
25. Farzad Z, Cochran AJ, McBride WH, Gray JD, Wong V, Morton DJ. Lymphocyte subset alterations in nodes regional to human melanoma. *Cancer Res* 1990; **50**: 3585–8.
26. de Gruijl TD, Bontkes HJ, Peccatori F, et al. Expression of CD3-zeta on T-cells in primary cervical carcinoma and in metastasis-positive and -negative pelvic lymph nodes. *Br J Cancer* 1999; **79**: 1127–32.
27. Shibuya TY, Nugyen N, McLaren CE, et al. Clinical significance of poor CD3 response in head and neck cancer. *Clin Cancer Res* 2002; **8**: 745–51.
28. Gastman BR, Atarshi Y, Reichert TE, et al. Fas ligand is expressed on human squamous cell carcinomas of the head and neck, and it promotes apoptosis of T lymphocytes. *Cancer Res* 1999; **59**: 5356–64.
29. Gastman BR, Johnson DE, Whiteside TL, Rabinowich H. Tumor-induced apoptosis of T lymphocytes: elucidation of intracellular apoptotic events. *Blood* 2000; **95**: 2015–23.
30. Verastegui E, Morales R, Barrera JL, et al. Immunological approach in the evaluation of regional lymph nodes of patients with squamous cell carcinoma of the head and neck. *Clin Immunol* 2002; **102**: 37–47.
31. Shibuya TY, Wei WZ, Zormeier M, et al. Anti-CD3/anti-CD28 bead stimulation overcomes CD3 unresponsiveness in patients with head and neck squamous cell carcinoma. *Arch Otolaryngol Head Neck Surg* 2000; **126**: 473–9.
32. Meneses A, Verastegui E, Barrera JL, de la Garza J, Hadden JW. Lymph node histology in head and neck cancer: impact of immunotherapy with IRX-2. *Int Immunopharmacol* 2003; **3**: 1083–91.

Acknowledgments

Supported in part by a grant from the Osaka Medical Research Foundation for Incurable Diseases. Authors thank Dr Cagri Delilbasi for comments and critical reading of the manuscript.